Chemistry Europe
European Chemical Societies Publishing

WILEY VCH

Excellence in Chemistry Research

Announcing our new flagship journal

- Gold Open Access
- Publishing charges waived
- Preprints welcome
- Edited by active scientists

Meet the Editors of *ChemistryEurope*

Luisa De Cola
Università degli Studi di Milano Statale, Italy

Ive Hermans
University of Wisconsin-Madison, USA

Ken Tanaka
Tokyo Institute of Technology, Japan

ChemCatChem

Research Article
doi.org/10.1002/cctc.202201672

Chemistry Europe
European Chemical Societies Publishing

www.chemcatchem.org

Polypyridine Iridium(III) and Ruthenium(II) Complexes for Homogeneous and Graphene-Supported Photoredox Catalysis

Alexandre Jacques[+],[a] Alexandre Devaux[+],[a] Christophe Rubay,[a] Florence Pennetreau,[a] Antonin Desmecht,[a] Koen Robeyns,[a] Sophie Hermans,*[a] and Benjamin Elias*[a]

Iridium(III) and ruthenium(II) polypyridyl based photocatalysts have been prepared and their structure determined using ^{1}H NMR, HR-MS and single crystal XRD. Their spectroscopic and electrochemical properties have been studied by UV-vis absorption, emission spectroscopy and cyclic voltammetry. These complexes have been used as photoredox homogeneous catalysts in an intramolecular cyclization model reaction in which they show high activity. They have been covalently anchored on graphene oxide (GO) *via* an esterification reaction and non-covalently fixed on reduced graphene oxide (rGO) *via* pyrene moieties. Heterogenized complexes exhibit good photocatalytic activities and, interestingly, the use of a pyrene-derivatized Ir(III) terpyridine-based complex highlights an unexpected "on/off" effect of the photocatalytic activity triggered by the presence or absence of rGO.

Introduction

Photochemistry has been recognized for many years as a powerful synthetic tool in organic chemistry.[1] It gained higher interest over the years with the development of new photoredox catalysts for specific organic transformations.[2] Plenty of reactions can now be achieved *via* photoredox catalysis, such as amine α-alkylations, radical cyclizations, cycloadditions and radical trifluoromethylations.[3] Nevertheless, these homogeneously catalyzed processes suffer from several drawbacks such as solvent compatibility, catalysts stability and the difficulty in recovering the catalysts at the end of a catalytic run. This has partially been solved using heterogeneous active photocatalysts such as TiO_2 or CdS but this alternative is not easily implemented when it comes to the use of transition metal complexes as photocatalysts, whose specificity is necessary for some complex reactions.[4] Polymeric systems with embedded catalytic complexes have also been reported but, despite their undeniable advantages, those systems are not commonly used due to their tedious preparation procedures, high cost and poor resistance to abrasion.[5]

One of the most common strategies to overcome the lack of homogeneous catalysts recovery is their heterogenization by tethering to the surface of a solid support. The first example of supported homogeneous photocatalyst for organic transformations was reported a few years ago.[6] This system consists in the anchoring of a $[Ru(bpy)_3]^{2+}$ (bpy = 2,2′-bipyridine) derivative onto silica and was proven to be highly efficient. However, the bipyridine ligands restrict the tuning possibilities of the supported photocatalyst due to the relatively difficult introduction of functional groups on bidentate pyridinic ligands. Yet the tuning of the ligand is, in this case, of paramount importance since it is necessary not only to coordinate the metal but also to connect the system to the solid surface, but it also sets the photophysical properties. The use of terpyridinic ligands, which are more easily derivatized,[7] can be envisaged to tackle this problem. Compared to $[Ru(tpy)_2]^{2+}$ (tpy = 2,2′:6′,2″-terpyridine) derivatives which have poor photocatalytic properties,[8] Iridium(III) bis-tpy complexes are better candidates due to their (*i*) remarkable photostability, (*ii*) long-lived excited state and (*iii*) ability to trigger photo-oxidative and/or photo-reductive charge transfers.[9] In addition, cyclometalated analogs can be easily obtained, *i.e.* the C/N ratio around the Ir(III) center can be tuned, having dramatic effect on their photoredox properties.[10] The inherent symmetry of the tpy prevents the formation of any geometrical isomers for the resulting complexes, offering a convenient way for unequivocal tethering and characterization of derivatized systems. In view of the above, we decided to develop a supported photocatalyst based on tpy ligands and Ir(III). There have been other reported examples of immobilized Ir(III) complexes in the recent literature, but solely based on cyclometalated analogs and mainly on polymer or silica supports.[11]

In the heterogenized catalysis field, a prominent place is occupied by carbonaceous solids.[12] Nano-forms of carbon have been heavily studied to be used as catalysts supports.[13–15] In particular, studies aiming at tethering catalysts onto graphene and graphene oxide have flourished within the past years[16] and photocatalysts make no exception.[17] However, most

[a] *Dr. A. Jacques,[+] Dr. A. Devaux,[+] C. Rubay, Dr. F. Pennetreau, Dr. A. Desmecht, Dr. K. Robeyns, Prof. S. Hermans, Prof. B. Elias*
Institute of Condensed Matter and Nanosciences,
Molecular Chemistry, Materials and Catalysis Division (IMCN/MOST)
Université catholique de Louvain (UCLouvain)
Place Louis Pasteur 1
1348 Louvain-la-Neuve (Belgium)
E-mail: sophie.hermans@uclouvain.be
benjamin.elias@uclouvain.be

[+] *These authors equally contributed to this work.*

Supporting information for this article is available on the WWW under https://doi.org/10.1002/cctc.202201672

examples presented in the literature are devoted to nanoparticles supported on graphene and the use of anchored complexes has been up to now scarcely described.

In this communication, we present (*i*) the synthesis of new pyrene derivatized Ir(III) bis-tpy complexes and a tris-bidentate Ru(II) complex for comparison purposes, (*ii*) the study of their spectroscopic and electrochemical properties, (*iii*) their use as homogeneous catalysts in a model photoredox cyclization reaction, (*iv*) their anchoring onto graphene-based materials and finally, (*v*) their use as heterogenized catalysts in the same reaction. The present study is one of the very first to report on an organic reaction photocatalyzed by a solid-supported homogeneous photocatalyst based on graphene materials, that play an active role, as will be shown below.

Results and Discussion

Firstly, the Ir(III) bis-tpy precursor complex (termed hereafter **[Ir-OH]$^{3+}$** – Figure 1) was synthesized following well-established methods.[18,19] It presents a benzylic alcohol moiety for further derivatization. Its structure was confirmed by ^{1}H NMR, high-resolution mass spectrometry (HR-MS) and single crystal X-ray diffraction (see SI). The spectroscopic and electrochemical properties of the complex have also been studied. All analytical data are available in the SI (see *e.g.* Table S3).

In view of its spectroscopic and electrochemical properties, **[Ir-OH]$^{3+}$** is a potentially suitable photocatalyst as it possesses four essential properties *i.e.* (*i*) absorption of visible light up to 470 nm (*ii*) long-lived excited state, (*iii*) high photostability and (*iv*) possibility of photo-induced electron transfer given the oxidation and reduction potentials of the excited state. To confirm this potentiality, **[Ir-OH]$^{3+}$** was used in the well-known photo-induced radical cyclization of dimethyl 2-bromo-2-(pent-4-en-1-yl)malonate **(1)** depicted in Scheme 1.[20] The results obtained with **[Ir-OH]$^{3+}$** and reference **[Ru(bpy)$_3$]$^{2+}$** complexes show a nearly full conversion and similar yields for both complexes, highlighting the photoredox catalytic efficiency of **[Ir-OH]$^{3+}$** (Table 1).

Further on, the benzylic alcohol function of **[Ir-OH]$^{3+}$** has been used to tether the catalyst both covalently and non-covalently onto graphene-based materials. On the one hand, graphene oxide (GO), bearing many oxygenated surface sites, can be covalently anchored by reaction between activated surface carboxylic acids and the benzylic alcohol function of **[Ir-OH]$^{3+}$**. On the other hand, non-covalent heterogenization by π - π stacking on reduced graphene-based material should be easily obtained using a pyrene derivatized complex. Figure 2 depicts the structure of several complexes we synthesized for the anchoring on graphene-based materials. Figure 2a shows **[Ir-IPr]$^{3+}$**, obtained with good yield by esterification of **[Ir-OH]$^{3+}$** with the corresponding acyl chloride in acetonitrile. **[Ir-IPr]$^{3+}$** will help to assess the photocatalytic activity of ester-containing complexes in the homogeneous phase in order to compare it with the heterogeneous covalent adducts. Figure 2b shows **[Ir-**

Table 1. Photocatalytic cyclization of **1** with **[Ir-OH]$^{3+}$** and **[Ru(bpy)$_3$]$^{2+}$**.[a]

Entry	Photocatalyst	Conv. [%][b]	Yield (X = H) [%][c]	Yield (X = Br) [%][c]
1	$[Ru(bpy)_3]^{2+}$	99	84	8
2	$[Ir\text{-}OH]^{3+}$	97	72	12

[a] 0.072 mmol (**1**), 1 mol% catalyst, 2 mL DMF, 12 equiv. Et_3N, under argon atmosphere, visible white light, 16 h. [b] Estimated by ^{1}H-NMR spectroscopy. [c] Isolated yield after purification by chromatography on SiO_2.

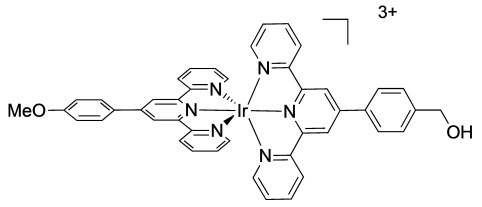

Figure 1. Structure of the **[Ir-OH]$^{3+}$** complex.

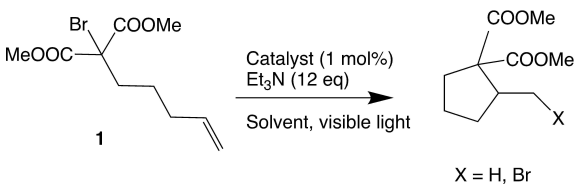

Scheme 1. Photocatalyzed radical cyclisation of malonate **(1)**.

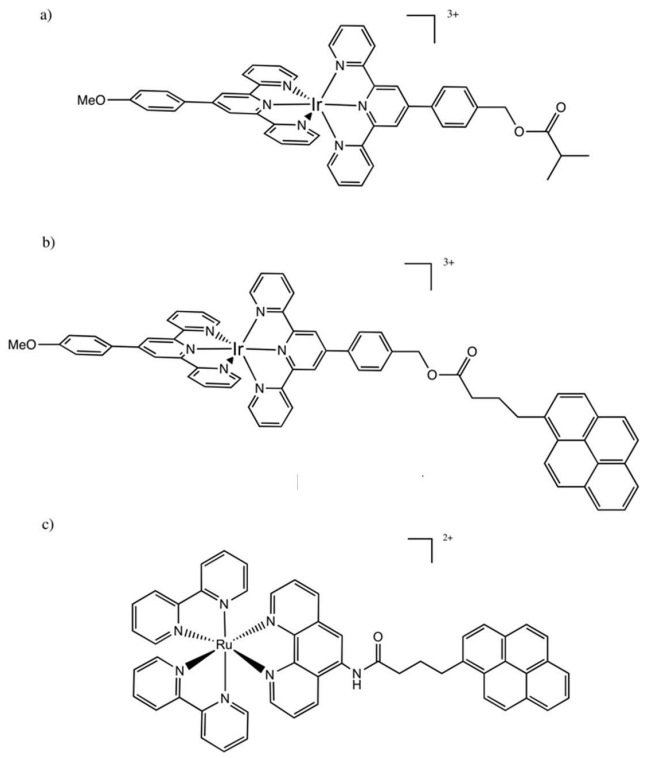

Figure 2. Structures of (a) **[Ir-IPr]$^{3+}$**, (b) **[Ir-Pyrene]$^{3+}$** and (c) **[Ru-Pyrene]$^{2+}$**.

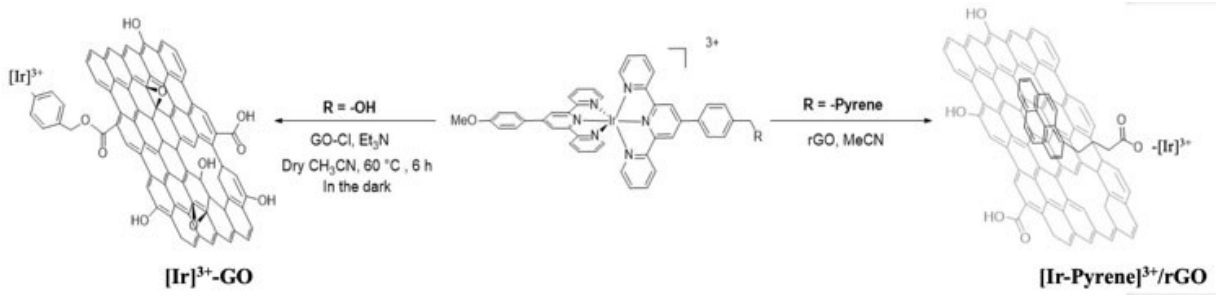

Scheme 2. Preparation of heterogeneous catalysts **[Ir]$^{3+}$-GO** and **[Ir-Pyrene]$^{3+}$/rGO**. The synthesis of **[Ru-Pyrene]$^{2+}$/rGO** follows the same protocol.

Pyrene]$^{3+}$ for which a low-resolution X-Ray structure was obtained (See SI), confirming the coupling of 1-pyrenebutyric acid to **[Ir-OH]$^{3+}$**. Figure 2c shows **[Ru-Pyrene]$^{2+}$**, a reference compound obtained from **[Ru(bpy)$_2$Cl$_2$]** and pyrene-derivatized 1,10-phenanthroline. These three species have been characterized by ^{1}H NMR and HR-MS, together with single crystal XRD structure for **[Ir-IPr]$^{3+}$**. Their spectroscopic and electrochemical properties were also measured (See SI). All Ir(III) complexes display very close spectroscopic data to the parent compound, evidencing the small influence of chemical modifications on the terpyridine unit on the complex properties.

The covalently anchored catalyst **[Ir]$^{3+}$-GO** was prepared by classical conversion of the carboxylic acid functions present at the GO surface into acyl chlorides (GO–Cl) followed by reaction of the latter with **[Ir-OH]$^{3+}$** (Scheme 2 – left). The non-covalently supported **[Ir-Pyrene]$^{3+}$/rGO** (or **[Ru-Pyrene]$^{2+}$/rGO**) was obtained by mixing **[Ir-Pyrene]$^{3+}$** (or **[Ru-Pyrene]$^{2+}$**) with rGO in acetonitrile and removal of the solvent (Scheme 2 – right). All experimental details are provided in the SI.

To confirm the presence of the iridium or ruthenium complexes on the carbonaceous surface, the supported catalysts were characterized by X-ray photoelectron spectroscopy (XPS). The presence of iridium and nitrogen in the **[Ir]$^{3+}$-GO** powder confirms the anchoring of the iridium complex on GO. The integrity of the complexes is highlighted by the measured values of N/Ir ratio (7.0 on GO) matching well with the theoretical value of 6 (See Table S4). In addition, the binding energy measured for Ir4f peak is in agreement with Ir(III) species,[21] further confirming the complex integrity (Figure S5). Concerning **[Ir-Pyrene]$^{3+}$/rGO** and **[Ru-Pyrene]$^{2+}$/rGO**, the measured values of N/Ir or N/Ru ratio are superior to the theoretical value (N/Ir ratio = 44; N/Ru ratio = 40; see Table S5), likely due to the presence of residual acetonitrile in the powder.

In the case of **[Ir]$^{3+}$-GO**, thermogravimetric analyses were carried out to confirm the covalent nature of the bond formed between complex and support. The high decomposition temperature ($T° > 600\,°C$) for the immobilized complex is a good clue to the covalent tethering of the iridium complex onto the graphene oxide surface (Figures S7–S8). In order to obtain a fully reliable quantification of the iridium content in the **[Ir]$^{3+}$-GO** solid, bulk elemental analysis has been performed by ICP.[22] The metal loading was found to be 1.23 wt% in the catalyst. This result is in good agreement with the TGA results, where mass losses might be attributed to graphene and organic components decomposition, leaving behind an Ir-only reside under air.

Regarding photochemical cyclization, the similar conversions obtained for **[Ir-IPr]$^{3+}$** (Table 2 – Entry 1) and **[Ir-OH]$^{3+}$** (Table 1 – Entry 2) indicate that the ester function does not have any impact on the photocatalytic activity. The cyclization was therefore carried out using heterogenized **[Ir]$^{3+}$-GO** as photocatalyst (Table 2 – Entry 2). The results show the appearance of cyclized product, highlighting the efficiency of the heterogenized photocatalyst. The lower conversion observed may result from a decrease in light absorption by the photocatalyst due to the presence of graphene-based material. Indeed, GO also absorbs photons emitted by the excitation lamp, reducing the concentration of the photocatalyst in the excited state. This is confirmed by a conversion decrease when GO is simply added to the homogeneous **[Ir-IPr]$^{3+}$** solution (Table 2 – Entry 3). It should also be mentioned that a conversion decrease by heterogenization of homogeneous catalysts is very often observed in the literature for other systems.[23] **[Ir-IPr]$^{3+}$** also showed good conversion in DCM, albeit slightly lower than in DMF presumably due to the lower solubility of Ir(III) complexes in this solvent (Table 2 – Entry 4). The reaction catalyzed by **[Ir]$^{3+}$-GO** in DCM displayed decreased conversion compared to the results obtained in DMF, similarly to the homogeneous case (Table 2 – Entry 5).

Concerning the non-covalent **[Ir-Pyrene]$^{3+}$/rGO** and **[Ru-Pyrene]$^{2+}$/rGO** photocatalysts, similarly to above, we first tested the homogeneous photocatalysts **[Ir-Pyrene]$^{3+}$** and **[Ru-Pyrene]$^{2+}$** to evaluate the influence of the pyrene tag on their photoredox catalytic properties. It should be mentioned that

Table 2. Photochemical cyclization of **(1)** with covalently immobilized catalysts and references for comparison [a].

Entry	Photocatalyst	Solvent	Conv. [%][b]
1	[Ir-IPr]$^{3+}$	DMF	97
2	[Ir]$^{3+}$-GO	DMF	52
3	[Ir-IPr]$^{3+}$ + GO	DMF	75
4	[Ir-IPr]$^{3+}$	DCM	89
5	[Ir] $^{3+}$-GO	DCM	34

[a] 0.072 mmol **(1)**, 1 mol% catalyst, 2 mL solvent, 12 equiv. Et_3N, under argon atmosphere, visible light, 16 h. [b] Estimated by ^{1}H-NMR spectroscopy.

Table 3. Photochemical cyclization of **(1)** with non-covalently immobilized catalysts and references for comparison [a]

Entry	Photocatalyst	Solvent[]	Conv. [%][b]
1	$[Ir\text{-}OH]^{3+}$	MeCN	90
2	$[Ir\text{-}Pyrene]^{3+}$	MeCN	0
3	$[Ru\text{-}Pyrene]^{2+}$	MeCN	66
4	$[Ir\text{-}Pyrene]^{3+}$/rGO	MeCN	32
5	$[Ru\text{-}Pyrene]^{2+}$/rGO	MeCN	17

[a] 0.072 mmol **(1)**, 1 mol% catalyst, 2 mL MeCN, 12 equiv. Et_3N, under argon atmosphere, visible light, 16 h. [b] Estimated by ^{1}H-NMR spectroscopy.

acetonitrile was used as the solvent for non-covalently supported catalysts because it solubilizes both the Ir(III) and Ru(II) complexes well. In addition, the high activity of the parent photocatalyst **[Ir-OH]$^{3+}$** is retained in this solvent (see Table 3 – Entry 1). While the ester function did not have any impact on the catalytic activity, the pyrene moiety completely inhibits the activity in the case of iridium compounds (Table 3 – Entry 2). This phenomenon might be explained by a photo-induced triplet energy transfer from the excited **[Ir]$^{3+}$** center to the pyrene unit, "switching off" the photocatalytic properties of the iridium center. This quenching process is in good agreement with the absence of luminescence observed for **[Ir-Pyrene]$^{3+}$** (See Table S3). Strikingly, using the heterogeneous **[Ir-Pyrene]$^{3+}$/rGO** system restores the catalytic efficiency (Table 3 – Entry 4). This suggests that the interactions between pyrene fragment and rGO prevent the "switching off" effect of the pyrene on the **[Ir]$^{3+}$** center. In other words, reduced graphene oxide has an indirect "switching on" effect on the **[Ir]$^{3+}$** photocatalyst. In contrast, as expected, the luminescent **[Ru-Pyrene]$^{2+}$** exhibits good photocatalytic conversion (Table 3 – Entry 3). Its adduct onto rGO shows moderate conversion (Table 3 – Entry 5), in agreement with lower light absorption in the presence of graphene-based materials (*vide supra*). All these results emphasize the great potential of graphene-supported photoredox catalysts in triggering and controlling photochemically induced complex reactions relevant to organic synthesis problems. Recycling of the **[Ir]$^{3+}$-GO** photocatalyst has also been tested. Evaporation of the solvent and washing off the remaining solid with MeOH to extract all organic molecules allowed to run the photocatalytic cyclization of **1** at least four times with the same batch of immobilized photocatalyst (see SI). Unfortunately, in the case of the heterogeneous **[Ir-Pyrene]$^{3+}$/rGO**, recycling studies showed a loss of activity, likely coming from some instability of the Ir moiety upon solid recovery. Indeed, it is known that pyrene/carbone surface interactions are dynamical and these complexes might be washed off during work up.[24]

Conclusions

In summary, three new Ir(III) bis-tpy complexes have been synthesized, namely **[Ir-OH]$^{3+}$**, **[Ir-IPr]$^{3+}$** and **[Ir-Pyrene]$^{3+}$** bearing an alcohol, ester and pyrene moiety respectively, as well as a tris-bidentate **[Ru-Pyrene]$^{2+}$** complex. These compounds were structurally, spectroscopically and electrochemically characterized and tested in the model photocatalyzed radical cyclization of malonate. **[Ir-OH]$^{3+}$** and **[Ir-IPr]$^{3+}$** show high photocatalytic activity, comparable to that of the well-known $[Ru(bpy)_3]^{2+}$ in homogenous conditions. When covalently anchored on graphene oxide, this photocatalytic activity in retained while the catalyst is heterogeneous. Strikingly, compared to **[Ru-Pyrene]$^{2+}$**, **[Ir-Pyrene]$^{3+}$** species does not exhibit any photocatalytic properties in the homogenous phase but a good activity when non-covalently immobilized on reduced graphene oxide. This complex and its heterogenized counterpart can therefore be seen as an "on/off" catalytic system, where graphene plays the dual role of support and on-switch. When recycling the immobilized systems, pyrene complexes were shown to be washed off during the work-up while the covalently immobilized photocatalysts could be recovered and reused multiple times.

Experimental Section

Materials

All chemicals were used as received unless otherwise stated in syntheses description. The synthesis of dimethyl 2-bromo-2-(pent-4-en-1-yl)malonate (1) has been carried out as reported in the literature.[20] Graphene oxide (GO) and reduced graphene oxide (rGO) were purchased from NanoInnova Technologies. The elemental analysis provided by the supplier gives: %C 51.25, %H 2.19; %N 0.31, %S 0.86, %O 43.99 for GO and %C 76.38, %H 1.44, %N 3.72 for reduced GO. The UV-VIS spectrum of GO exhibits a maximum absorption peak at about 223 nm, corresponding to π-π* transition of aromatic C=C bonds. The absorption peak for reduced GO is red shifted to 270 nm. This phenomenon of red shift has been used as a monitoring tool for the reduction of GO. rGO presents a Specific Surface Area of 103.2 m^2/g.

Synthetic procedures and characterization

[Ir-OH](3PF$_6$)[18,19]

A suspension of [(4′-MeO-Phtpy)$IrCl_3$] (58 mg, 0.091 mmol) and 4′-CH_2OH-Phtpy (34 mg, 0.100 mmol) was heated to 170 °C in degassed ethylene glycol (2 mL) in the dark under argon for 30 min. After cooling, aqueous NH_4PF_6 was added to yield the crude solid product. The pure product was isolated by column chromatography on Al_2O_3 (acetone/water, from 100/0 to 90/10), which yielded the complex as a yellow solid (115 mg, 97%). ^{1}H NMR (CD_3CN, 300 MHz) : δ (ppm), 9.09 (s, 2H, $H_{3'}$ and $H_{5'}$ of tpy-C_6H_4-CH_2OH), 9.04 (s, 2H, $H_{3'}$ and $H_{5'}$ of tpy-C_6H_4-OMe), 8.72 (d, 4H, H_3 and $H_{3''}$ of both tpys, $J_{H3\text{-}H4}$ = 8.0 Hz), 8.25–8.18 (m, 8H, H_4 and $H_{4''}$ of both tpys, H_b of tpy-C_6H_4-OMe and H_b of tpy-C_6H_4-CH_2OH), 7.78 (d, 2H, H_a of tpy-C_6H_4-CH_2OH, $J_{Ha\text{-}Hb}$ = 8.4 Hz), 7.71–7.68 (m, 4H, H_6 and $H_{6''}$ of both tpys), 7.48 (m, 4H, H_5 and $H_{5''}$ of both tpys), 7.34 (d, 2H, H_a of tpy-C_6H_4-OMe, $J_{Ha\text{-}Hb}$ = 8.9 Hz), 4.82 (d, 2H, CH_2-OH, $J_{CH2\text{-}OH}$ = 5.6 Hz), 4.00 (s, 3H, OMe), 3.49 (t, 1H, -OH, $J_{HO\text{-}CH2}$ = 5.7 Hz). HRMS (ESI): m/z calculated for $[C_{44}H_{34}N_6O_2{}^{193}IrP_2F_{12}]^+$, 1161.1651; found: 1161.1657, m/z calculated for $[C_{44}H_{34}N_6O_2{}^{193}IrPF_6]^{2+}$, 508.1002; found: 508.1005, m/z calculated for $[C_{44}H_{34}N_6O_2{}^{193}Ir]^{3+}$, 290.4119; found: 290.4119.

[Ir-IPr](3PF$_6$)

To [Ir-OH](3PF$_6$) (25 mg, 0.019 mmol) and Et_3N (0.416 mL, 3.80 mmol) dissolved in dry acetonitrile (8 mL) was added isobutyryl chloride (0.202 mL, 203 mg, 1.90 mmol) at room temperature under argon. The reaction was stirred for 16 h. Aqueous saturated KPF_6 (2 mL) was added to quench the reaction and the solvent was removed. The yellow powder was washed with water, EtOH and Et_2O. Recrystallization using CH_3CN-THF yielded the pure complex as a yellow solid (18 mg, 69%). RMN ^{1}H (CD_3CN, 300 MHz) : δ (ppm), 9.08 (s, 2H, $H_{3'}$ and $H_{5'}$ of tpy-C_6H_4-$CH_2OCOCH(CH_3)_2$), 9.04 (s, 2H, $H_{3'}$ and $H_{5'}$ of tpy-C_6H_4-OMe), 8.71 (d, 2H, H_3 and $H_{3''}$ of tpy-C_6H_4-OMe, $J_{H3\text{-}H4}$ = 7.5 Hz), 8.70 (d, 2H, H_3 and $H_{3''}$ of tpy-C_6H_4-$CH_2OCOCH(CH_3)_2$, $J_{H3\text{-}H4}$ = 7.5 Hz) 8.25–8.19 (m, 8H, H_4 and $H_{4''}$ of both tpys, H_b of both tpys), 7.79 (d, 2H, H_a of tpy-C_6H_4-$CH_2OCOCH(CH_3)_2$, $J_{Ha\text{-}Hb}$ = 8.4 Hz), 7.69 (dd, 2H, H_6 and $H_{6''}$ of tpy-C_6H_4-OMe, $J_{H6\text{-}H5}$ = 5.7 Hz, $J_{H6\text{-}H4}$ = 0.9 Hz), 7.68 (dd, 2H, H_6 and $H_{6''}$ of tpy-C_6H_4-$CH_2OCOCH(CH_3)_2$, $J_{H6\text{-}H5}$ = 5.7 Hz, $J_{H6\text{-}H4}$ = 0.9 Hz), 7.49–7.46 (m, 4H, H_5 and $H_{5''}$ of both tpys), 7.34 (d, 2H, H_a of tpy-C_6H_4-OMe, $J_{Ha\text{-}Hb}$ = 8.9 Hz), 5.32 (s, 2H, CH_2), 4.00 (s, 3H, OMe), 2.70 (s, 6H, –$(CH_3)_2$Br). HRMS (ESI): m/z calculated for $[C_{48}H_{40}N_6O_3{}^{193}IrP_2F_{12}]+$, 1231.2069; found: 1231.2075, m/z calculated for $[C_{48}H_{40}N_6O_3{}^{193}IrPF_6]^{2+}$, 543.1211; found: 543.1215, m/z calculated for $[C_{48}H_{40}N_6O_3{}^{193}Ir]^{3+}$, 313.7592; found: 313.7590.

[Ir-Pyrene](3PF$_6$)

To [Ir-OH](3PF$_6$) (30 mg, 0.023 mmol) dissolved in dry acetonitrile (8 mL) was successively added 1-pyrenebutyric acid (7 mg, 0.025 mmol), dimethylaminopyridine (DMAP) (1 mg, 0.007 mmol) and N,N′-dicyclohexylcarbodiimide (DCC) (5 mg, 0.025 mmol) at room temperature under argon. The reaction mixture was stirred for 16 h. An excess of tetrabutylammonium chloride (tBu_4NCl) was added to precipitate the crude product. After filtration, the solid was purified by column chromatography on SiO_2 (Eluent: CH_3CN/H_2O/KNO_3aq (90/9/1)) to afford an orange powder (16 mg, 44%). RMN ^{1}H (CD_3CN, 500 MHz) : δ (ppm), 9.05 (s, 2H, $H_{3'}$ and $H_{5'}$ of tpy-C_6H_4-$CH_2OCO(CH_2)_3$-Pyrene), 9.04 (s, 2H, $H_{3'}$ and $H_{5'}$ of tpy-C_6H_4-OMe), 8.72 (d, 2H, H_3 and $H_{3''}$ of tpy-C_6H_4-OMe, $J_{H3\text{-}H4}$ = 7.5 Hz), 8.66 (d, 2H, H_3 and $H_{3''}$ of tpy-C_6H_4-$CH_2OCO(CH_2)_3$-Pyrene, $J_{H3\text{-}H4}$ = 7.5 Hz), 8.40 (d, 1H, H_{pyr}, $J_{Hpyr\text{-}Hpyr}$ = 9.3 Hz), 8.27-8.17 (m, 12H, H_4 and $H_{4''}$ of both tpys, H_b of both tpys, H_{pyr}), 8.14 (d, 1H, H_{pyr}, $J_{Hpyr\text{-}Hpyr}$ = 9.0 Hz), 8.11 (d, 1H, H_{pyr}, $J_{Hpyr\text{-}Hpyr}$ = 9.0 Hz), 8.02 (t, 1H, H_{pyr}, $J_{Hpyr\text{-}Hpyr}$ = 7.7 Hz), 7.99 (d, 1H, H_{pyr}, $J_{Hpyr\text{-}Hpyr}$ = 7.7 Hz), 7.80 (d, 2H, H_a of tpy-C_6H_4-$CH_2OCO(CH_2)_3$-Pyrene, $J_{Ha\text{-}Hb}$ = 8.3 Hz), 7.70 (dd, 2H, H_6 and $H_{6''}$ of tpy-C_6H_4-OMe, $J_{H6\text{-}H5}$ = 5.7 Hz, $J_{H6\text{-}H4}$ = 0.9 Hz), 7.68 (dd, 2H, H_6 and $H_{6''}$ of tpy-C_6H_4-$CH_2OCO(CH_2)_3$-Pyrene, $J_{H6\text{-}H5}$ = 5.7 Hz, $J_{H6\text{-}H4}$ = 0.9 Hz), 7.53–7.47 (m, 4H, H_5 and $H_{5''}$ of both tpys), 7.37 (d, 2H, H_a of tpy-C_6H_4-OMe, $J_{Ha\text{-}Hb}$ = 8.9 Hz), 5.35 (s, 2H, CH_2), 4.02 (s, 3H, OMe), 3.46 (t, 2H, CH_2, $J_{CH2\text{-}CH2}$ = 7.9 Hz), 2.65 (t, 2H, CH_2, $J_{CH2\text{-}CH2}$ = 7.1 Hz), 2.27–2.20 (m, 2H, CH_2). HRMS (ESI): m/z calculated for $[C_{64}H_{48}N_6O_3{}^{193}IrP_2F_{12}]^+$, 1431.2695; found: 1431.2694, m/z calculated for $[C_{64}H_{48}N_6O_3{}^{193}IrPF_6]^{2+}$, 643.1524; found: 643.1525, m/z calculated for $[C_{64}H_{48}N_6O_3{}^{193}Ir]^{3+}$, 380.4467; found: 380.4468.

[Ir]$^{3+}$-GO

Graphene oxide (NanoInnova GO, 350 mg) was introduced in a round bottom flask with $SOCl_2$ (20 mL) and DMF (0.5 ml). The suspension was sonicated for 15 minutes and heated in an oil bath at 70 °C for 24 hours. The suspension was then centrifuged for 10 minutes at 4000 rpm (Universal 320 – Hettich Zentrifugen). The supernatant was removed and the solid filtered (on filters GVWP, PVDF, pores 0.22 μm, Millipore) and washed with THF (800 mL).

The so-obtained chlorinated graphene oxide (160 mg) was introduced in a schlenk round bottom flask. Dry acetonitrile (20 mL) was added under argon and the suspension was sonicated for 10 minutes. [Ir-OH]$^{3+}$ (83 mg) and distilled triethylamine (0.2 mL) were added. The schlenk flash was wrapped with an aluminum foil and heated at 60 °C for 6 hours. The solid was then purified by filtration (on filters GVWP, PVDF, pores 0.22 μm, Millipore) and washed with acetonitrile (950 mL) and diethyl ether (250 mL). The purification is performed in the dark.

Phen-Pyrene

5-amino-1,10-phenanthroline (0.35 mmol, 1 equiv.) and 1-pyrenebutanoyl chloride (0.035 mmol, 1 equiv.) were dissolved in 10 mL dichloromethane (DCM) separately and mixed slowly together. The mixture was stirred at room temperature for 3 hours and the product precipitated upon stirring. The precipitate was filtered and washed with 20 mL DCM. The crude product was used in the next step without any further purification. The crude product is a dark-red solid.

[Ru-Pyrene](2PF$_6$)

[Ru(bpy)$_2$Cl$_2$] (0.049 mmol, 1 equiv.) and Phen-Pyrene (0.049 mmol, 1 equiv.) were dissolved in 8 mL EtOH/$CHCl_3$ (1/1). The mixture was stirred at 70 °C for 6 hours. Aqueous saturated KPF_6 (4 mL) was added to quench the reaction and the solvent was removed under vacuum. The solid was purified by column chromatography on SiO_2 (Eluent: CH_3CN/H_2O/KNO_3aq (90/9/1)) to afford an orange powder (27%). RMN ^{1}H (CD3CN, 500 MHz) : δ (ppm), 8.76 (s, 1H, H_B), 8.55–8.41 (m, 8H, $H_{C\text{ or }D,\ C'\text{ or }D',\ 5,\ 5',\ 6,\ 6',\ H}$), 8.20–7.96 (m, 13H, $H_{C\text{ or }D,\ C'\text{ or }D',\ 2,\ 2',\ 9,\ 9',\ H}$), 7.82 (t, 2H, $H_{3,\ 3'\text{ or }8,\ 8'}$, J = 5.6 Hz), 7.65 (dd, 1H, $H_{A\text{ or }A'}$, $J_{A\text{-}C\text{ or }A'\text{-}C'}$ = 5.20 Hz, $J_{A\text{-}D\text{ or }A'\text{-}D'}$ = 3.20 Hz), 7.61 (dd, 1H, $H_{A\text{ or }A'}$, $J_{A\text{-}C\text{ or }A'\text{-}C'}$ = 5.20 Hz, $J_{A\text{-}D\text{ or }A'\text{-}D'}$ = 3.30 Hz), 7.53 (t, 2H, $H_{3,\ 3'\text{ or }8,\ 8'}$, J = 5.6 Hz), 7.44 (m, 2H, $H_{4,\ 4'\text{ or }7,\ 7'}$), 7.23 (m, 2H, $H_{4,\ 4'\text{ or }7,\ 7'}$), 3.53 (t, 2H, H_G, $J_{G\text{-}F}$ = 7.50 Hz), 2.73 (t, 2H, H_E, $J_{E\text{-}F}$ = 7.30 Hz), 2.35 (quint., 2H, H_F, J = 7.50 Hz). HRMS (HRMS): m/z calculated for $[C_{52}H_{39}N_7O^{102}RuPF_6]^+$, 1024.1896; found: 1024.19079, m/z calculated for $[C_{52}H_{39}N_7O^{102}Ru]^{2+}$, 439.6129; found: 439.6130.

Preparation of [Ir-Pyrene]$^{3+}$/rGO or [Ru-Pyrene]$^{2+}$/rGO

50 mg of rGO (NanoInnova) were added to [Ir-Pyrene](PF$_6$)$_3$ or [Ru-Pyrene](PF$_6$)$_2$ (5 mg) dissolved in 5 mL of MeCN. The mixture was stirred in an ultrasonic bath. After 5 minutes, the mixture was concentrated and dried under vacuum. The black powder was washed 2 times with MeOH before being used for the photoredox catalysis experiments.

General procedure for homogeneous photoredox catalysis

Under argon atmosphere, the photocatalyst (1 mol%, 0.72 μmol), Et_3N (116 μL, 0.864 mol) and bromomalonate (1) (20 mg, 0.072 mmol) were dissolved in 2 mL of the appropriate solvent, previously degassed by freeze-pump-thaw procedure. The resulting mixture was stirred under light irradiation of three blue LED lamps (output power : 3 W; $\lambda_{max\ irradiation}$ = 415 nm). After 16 h, 30 mL of diethylether and 30 mL of water were added to the mixture. The two layers were separated and the aqueous phase was extracted 2 times with 20 mL of diethylether. All organic phases were combined, washed 3 times with 30 mL of water, dried over $MgSO_4$ and concentrated under vacuum. The resulting solid was purified by column chromatography on SiO_2 (Eluent: Cyclohexane/AcOEt (85/15)) to afford the pure product. The desired fractions were collected and evaporated under reduced pressure to afford the cyclized product as a colorless oil. Yields were determined by ^{1}H

NMR spectroscopy using 3,4,5-trimethoxybenzaldehyde as internal reference ($CDCl_3$, 500 MHz, relaxation delay of 20 seconds).

General procedure for heterogeneous photoredox catalysis with $[Ir]^{3+}$-GO

Under argon atmosphere, the photocatalyst (1 mol% of Ir(III), 0.72 μmol of Ir(III)), Et_3N (116 μL, 0.864 mol) and bromomalonate (1) (20 mg, 0.072 mmol) were dissolved in 2 mL of the appropriate solvent, previously degassed by freeze-pump-thaw procedure. The resulting mixture was stirred under light irradiation of three blue LED lamps (output power : 3 W; $\lambda_{max\ irradiation} = 415$ nm). After 16 h, the photocatalyst material was recovered by filtration and washed 3 times with 20 mL of diethylether. The filtrate and the ether phases were combined, washed 3 times with 30 mL of water, dried over $MgSO_4$ and concentrated under vacuum. The resulting solid was purified by column chromatography on SiO_2 (Eluent: Cyclohexane/AcOEt (85/15)) to afford the pure product.

General procedure for heterogeneous photoredox catalysis with $[Ir\text{-}Pyrene]^{3+}$/rGO or $[Ru\text{-}Pyrene]^{2+}$/rGO

Under argon atmosphere, the photocatalyst (1 mol% of Ir(III)/Ru(II), 0.72 μmol of Ir(III)/Ru(II)), Et_3N (116 μL, 0,864 mol) and bromomalonate (1) (20 mg, 0,072 mmol) were dissolved in 2 mL of MeCN previously degassed by freeze-pump-thaw procedure. The resulted mixture was stirred under light irradiation of three blue LED lamps (output power: 3 W; $\lambda_{max\ irradiation} = 415$ nm). After 16 h, the solvent was removed under vacuum. The black powder was washed 3 times with 5 mL of MeOH. The alcohol phases were combined and concentrated under vacuum. The resulting solid was purified by column chromatography on SiO_2 (Eluent: Cyclohexane/AcOEt (85/15)) to afford the pure product.

Acknowledgements

The authors acknowledge FRS-FNRS, FRIA, Fédération Wallonie-Bruxelles, Loterie Nationale, Université catholique de Louvain and the Prix Pierre et Colette Bauchau for financial support. We are also grateful to L. Marcelis and A. Aydogan for their scientific help.

Conflict of Interest

The authors declare no competing interest.

Data Availability Statement

The data that support the findings of this study are available in the supplementary material of this article.

Keywords: graphene · iridium · photocatalysis · photochemistry · supported catalysts

[1] T. Bach, J. P. Hehn, *Angew. Chem. Int. Ed.* **2011**, *50*, 1000–1045; *Angew. Chem.* **2011**, *123*, 1032–1077.
[2] C. K. Prier, D. A. Rankic, D. W. C. MacMillan, *Chem. Rev.* **2013**, *113*, 5322–5363.
[3] Y. Xi, H. Yi, A. Lei, *Org. Biomol. Chem.* **2013**, *11*, 2387–2403.
[4] a) M. Rueping, J. Zoller, D. C. Fabry, K. Poscharny, R. M. Koenigs, T. E. Weirich, J. Mayer, *Chem. Eur. J.* **2012**, *18*, 3478–3481; b) T. Mitkina, C. Stanglmair, W. Setzer, M. Gruber, H. Kisch, B. König, *Org. Biomol. Chem.* **2012**, *10*, 3556–3561.
[5] a) Z. Xie, C. Wang, K. E. deKrafft, W. Lin, *J. Am. Chem. Soc.* **2011**, *133*, 2056–2059; b) H. Shimakoshi, M. Nishi, A. Tanaka, K. Chikama, Y. Hisaeda, *Chem. Commun.* **2011**, *47*, 6548–6550.
[6] G. J. Barbante, T. D. Ashton, E. H. Doeven, F. M. Pfeffer, D. J. D. Wilson, L. C. Henderson, P. S. Francis, *ChemCatChem* **2015**, *7*, 1655–1658.
[7] A. M. W. C. Thompson, *Coord. Chem. Rev.* **1997**, *160*, 1–52.
[8] S. Campagna, F. Puntoriero, F. Nastasi, G. Bergamini, V. Balzani, *Top. Curr. Chem.* **2007**, *280*, 117–214.
[9] a) A. Jacques, A Kirsch-De Mesmaeker, B. Elias, *Inorg. Chem.* **2014**, *53*, 1507–1512; b) C. Lentz, L. Marcélis, L. Troian-Gautier, K. Robeyns, E. Cauët, B. Elias, *Journal of Photochemistry & Photobiology, A: Chemistry 405* **2021**, 112957.
[10] a) G. R. Freeman, J. A. G. Williams, *Top. Organomet. Chem.* **2013**, *40*, 89–130; b) R. Bevernaegie, S. A. M. Wehlin, B. Elias, L. Troian-Gautier *ChemPhotoChem* **2021**, *5*, 217–234.
[11] A. A. Yakushev, A. S. Abel, A. D. Averin, I. P. Beletskaya, A. V. Cheprakov, I. S. Ziankou, L. Bonneviot, A. Bessmertnykh-Lemeune, *Coord. Chem. Rev.* **2022**, *458*, 214331–214412.
[12] P. Serp, J. L. Figueiredo in *Carbon Materials for Catalysis*, John Wiley & Sons, Inc., Hoboken New Jersey, **2009**.
[13] A. Schaetz, M. Zeltner, W. J. Stark, *ACS Catal.* **2012**, *2*, 1267–1284.
[14] N. M. Julkapli, S. Bagheri, *Int. J. Hydrogen Energy* **2015**, *40(2)*, 948–979.
[15] a) D. S. Su, S. Perathoner, G. Centi, *Chem. Rev.* **2013**, *113*, 5782–5816; b) Y. Yan, J. Miao, Z. Yang, F.-X. Xiao, H. B. Yang, B. Liu, Y. Yang, *Chem. Soc. Rev.* **2015**, *44*, 3295–3346.
[16] a) B. F. Machado, P. Serp, *Catal. Sci. Technol.* **2012**, *2*, 54–75; b) S. Navalon, A. Dhakshinamoorthy, M. Alvaro, H. Garcia, *Coord. Chem. Rev.* **2016**, *312*, 99–148 ; c) D. Marquardt, F. Beckert, F. Pennetreau, F. Tölle, R. Mülhaupt, O. Riant, S. Hermans, J. Barthel, C. Janiak, *Carbon* **2014**, *66*, 285–294; d) M. Masteri-Farahani, M. Modarres, *Colloids Surf. A* **2017**, *529*, 886–892.
[17] a) X. An, J. C. Yu, *RSC Adv.* **2011**, *1*, 1426–1434; b) Q. Xiang, Ji. Yu, M. Jaroniec, *Chem. Soc. Rev.* **2012**, *41*, 782–796; c) M.-Q. Yang, Y.-J. Xu, *Phys. Chem. Chem. Phys.* **2013**, *15*, **19102–19118**; d) R. K. Upadhyay, N. Soin, S. S. Roy, *RSC Adv.* **2014**, *4*, 3823–3851; e) Y. Luo, G. Chang, L. Huang, L. Zhang, J. Cui, X. Zhu, S. Xu, *ChemistrySelect* **2021**, *6 (8)*, 1929–1936.
[18] D. C. Goldstein, Y. Y. Cheng, T. W. Schmidt, M. Bhadbhade, P. Thordarson, *Dalton Trans.* **2011**, *40*, 2053–2061.
[19] J.-P Collin, I. M. Dixon, J.-P. Sauvage, J. A. G. Williams, F. Barigelletti, L. Flamigni, *J. Am. Chem. Soc.* **1999**, *121*, 5009–5016.
[20] J. M. R. Narayanam, C. R. J. Stephenson, *Chem. Soc. Rev.* **2011**, *40*, 102–113.
[21] a) J. A. Bearden, A. F. Burr, *Rev. Mod. Phys.* **1967**, *39*, 125–142; b) B. D. El-Issa, A. Katrib, R. Ghodsian, B. A. Salsa, S. H. Addassi, *Int. J. Quantum Chem.* **1988**, *33*, 195–216; c) S. Le Vot, L. Roué, D. Bélanger, *Electrochim. Acta* **2012**, *59*, 49–56.
[22] Note that bulk elemental analysis was not necessary for **$[Ir\text{-}Pyrene]^{3+}$/rGO** nor **$[Ru\text{-}Pyrene]^{2+}$/rGO** as no filtration step was required for their preparation. The precise amount of iridium or ruthenium present in the final solid is simply equal to the amount of iridium or ruthenium introduced in the flask.
[23] a) A. A. Keterling, A. S. Lisitsyn, V. A. Likholobov, A. A. Gall', A. S. Trachum, *Kinet. Catal.* **1991**, *31*, 1273–1277; b) A. Corma, H. Garcia, *Adv. Synth. Catal.* **2006**, *348*, 1391–1412; c) C. Copéret, J.-M. Basset, *Adv. Synth. Catal.* **2007**, *349*, 78–92.
[24] C. Vriamont, M. Devillers, O. Riant, S. Hermans, *Chem. Eur. J.* **2013**, *19*, 12009–12017.

Manuscript received: December 23, 2022
Revised manuscript received: January 22, 2023
Version of record online: February 9, 2023